

REPORT DOCUMENTATION PAGE				<i>Form Approved</i> OMB No. 0704-0188	
<p>The public reporting burden for this collection of information is estimated to average 1 hour per response, including the time for reviewing instructions, searching existing data sources, gathering and maintaining the data needed, and completing and reviewing the collection of information. Send comments regarding this burden estimate or any other aspect of this collection of information, including suggestions for reducing the burden, to Department of Defense, Washington Headquarters Services, Directorate for Information Operations and Reports (0704-0188), 1215 Jefferson Davis Highway, Suite 1204, Arlington, VA 22202-4302. Respondents should be aware that notwithstanding any other provision of law, no person shall be subject to any penalty for failing to comply with a collection of information if it does not display a currently valid OMB control number.</p> <p>PLEASE DO NOT RETURN YOUR FORM TO THE ABOVE ADDRESS.</p>					
1. REPORT DATE (DD-MM-YYYY) 30-04-2007		2. REPORT TYPE Final		3. DATES COVERED (From - To) 20-06-2005 to 07-03-2007	
4. TITLE AND SUBTITLE Microbial Fuel Cells with High Power and High Energy Density			5a. CONTRACT NUMBER FA520905P0505		
			5b. GRANT NUMBER		
			5c. PROGRAM ELEMENT NUMBER		
6. AUTHOR(S) Dr. Changming Li			5d. PROJECT NUMBER		
			5e. TASK NUMBER		
			5f. WORK UNIT NUMBER		
7. PERFORMING ORGANIZATION NAME(S) AND ADDRESS(ES) Nanyang Technological University N1.3-B2-12, 70 Nanyang Dr. Singapore 637457 Singapore			8. PERFORMING ORGANIZATION REPORT NUMBER N/A		
9. SPONSORING/MONITORING AGENCY NAME(S) AND ADDRESS(ES) AOARD UNIT 45002 APO AP 96337-5002			10. SPONSOR/MONITOR'S ACRONYM(S) AOARD		
			11. SPONSOR/MONITOR'S REPORT NUMBER(S) AOARD-054073		
12. DISTRIBUTION/AVAILABILITY STATEMENT Approved for public release; distribution is unlimited.					
13. SUPPLEMENTARY NOTES					
14. ABSTRACT This report covers investigations of advanced microbial H ₂ /O ₂ -fuel cell development, miniaturization, and energy and power density enhancement. The anode is very important in the performance of a microbial fuel cell (MFC), and is often the limiting factor for a high power output. In present work, we used the CNT/PANI composite as the anode materials of MFCs for the first time and investigated the electrocatalytic properties of the composite associated with the bacterium biocatalyst. A method was developed to fabricate a nanostructured CNT/PANI composite anode for MFCs.					
15. SUBJECT TERMS MEMS, PowerMEMS, BioNano Systems					
16. SECURITY CLASSIFICATION OF:			17. LIMITATION OF ABSTRACT	18. NUMBER OF PAGES	19a. NAME OF RESPONSIBLE PERSON
a. REPORT	b. ABSTRACT	c. THIS PAGE			David Sonntag, LtCol, USAF
U	U	U	UU	22	19b. TELEPHONE NUMBER (Include area code) +81-3-5410-4409

Final Report

AOARD-05-4073

**Advanced Microbial Fuel Cell
Development, Miniaturization and
Energy and
Power Density Enhancement**

Chang Ming Li

School of Chemical and Biomedical Engineering

Nanyang Technological University

Singapore

Abstract

The purpose of the project was to develop an advanced microbial fuel cell (MFC) with miniaturization, and energy and power density enhancement. Anode is very important in the performance of a MFC, and is often the limiting factor for a high power output. In present work, we used the CNT/PANI composite as the anode materials of MFCs for the first time and investigated the electrocatalytic properties of the composite associated with the bacterium biocatalyst. A method was developed to fabricate a nanostructured CNT/PANI composite anode for MFCs. In our experiments, anaerobic cultured *Escherichia coli K12* was used as the biological catalyst and glucose was used as the organic substrate for the anode-limiting MFC cell. Fourier transform infrared spectroscopy (FTIR) and scanning electron microscopy (SEM) were employed to characterize the chemical composition and morphology of the plain PANI and CNT/PANI composite. The result proved that the specific surface area of the composite was much larger than the plain polymer. Therefore, it could be expected that the structure difference of these materials could result in different discharge profile and impedance spectra of the anodes made by these materials. The electrocatalytic behavior of the composite anode for MFCs was investigated with electrochemical impedance spectra (EIS) and discharge experiments. The result revealed that the composite anode not only improved the electrode conductivity and specific surface area, but also provided unique active centers, possibly due to its specific nanostructure. The current generation profile and constant current discharge curves of the anodes made from plain PANI, 1% wt and 20% wt CNT in the CNT-PANI composites, respectively, revealed that the performance of the composite anodes were much better than the plain polymer. The 20% wt CNT composite anode had the highest electrochemical activity and its maximum power density could achieve 42 mW m^{-2} with *E. coli* as the microbial catalyst. In comparison to the reported performance of different anodes used in *E. coli*-based MFCs, the CNT/PANI composite anode was excellent, and could significantly improve the energy density and power density for miniaturized systems, which could lead to great potential in MFC applications.

1 Introduction

MFCs use bacteria as the catalysts to oxidize organic and inorganic matter for energy generation. A number of factors affect MFC performance including microbial inoculums, chemical substrate, proton exchange material (or absence of this material), cell internal and external resistance, solution ionic strength, electrode materials and electrode spacing [1-3]. Among these factors, a high performance electrode material is most essential. To improve the power output of MFCs, a lot of researchers focus on the cathode modification and bacteria inoculums optimization [4, 5]. However, anode is also important in the performance of a MFC, and is often the limiting factor for a high power output. The anode material and its structure could directly affect the bacteria attachment, electron transfer and substrate oxidation. Up to date, carbon materials such as carbon cloth and carbon paper are applied in most of MFC anodes due to its stability in a microbial inoculum mixture, high conductivity and high specific surface area. Nevertheless, they have no considerable electrocatalysis for the anode microbial reactions and thus the modification of carbon material is the main approach for improving their performance. There is a great need to develop a new-type anode material for MFCs, which is more advantageous than regular carbon cloth and carbon papers.

The CNT is a unique member of the nanostructured carbon materials, which has shown very promising properties as the catalyst support for fuel cell applications due to their unique electrical and structural properties [6]. CNTs were superior to carbon blacks as catalyst supports for proton exchange membrane fuel cells (PEMFCs) [7, 8]. They were also served as anode materials for enzymatic biofuel cells [9, 10]. However, it was reported that CNT had cellular toxicity that could lead to proliferation inhibition and cell death [11, 12]. Thus, it was not suitable for MFCs unless it was modified to reduce the cellular toxicity.

Conductive polymers have attracted intensive research in different electrochemical devices

[13-15]. PANI is one of the important conducting polymers due to its relatively facile process ability, electrical conductivity, and environmental stability. The electronic properties of PANI can be reversibly controlled by both doping/dedoping and protonation process, in which its emeraldine base and emeraldine salt form can be interchanged [16]. It was reported that PANI was used to detect microorganism such as *E. coli* with enzyme based method [17, 18]. Uwe et al employed PANI to modify platinum electrode as the anode of MFC. They accomplished a current output more than one order of magnitude larger than the known MFCs [19]. The conductive PANI used in the MFC not only has a protective function for bacteria, but also directly contributes to electrocatalysis with a high current density [19, 20]. However, the lower conductivity and poor electron transfer of PANI limit its application in MFCs.

The fabrication of CNT/PANI composites has received great interest in recent years since the incorporation of CNTs into PANI can result in new composite materials with enhanced electronic properties. For example, Wallace et al. reported that the PANI fibers containing CNTs exhibited significant improvement in mechanical strength and conductivity [21]. Liu et al. constructed CNT/PANI multilayer films through the layer-by-layer assembly method, and the CNTs inside the multilayer film could expand the electroactivity of PANI to a neutral electrolyte [22]. Thus, the enhanced conductive CNT/PANI composite could possibly be used in MFCs for performance improvement. However, the electrocatalytic behavior and application of the CNT/PANI composite in MFCs has not been studied. In this report, we used the CNT/PANI composite as the anode of MFCs for the first time and investigated the electrocatalytic properties of the composite associated with the bacterium biocatalyst. A method was developed to fabricate a nanostructured CNT/PANI composite anode for MFCs. In our experiments, anaerobic cultured *Escherichia coli K12* was used as the biological catalyst and glucose was used as the organic substrate for the anode-limiting MFC cell. The discharge performance of the CNT/PANI anode in the testing MFC was evaluated with the beaker MFC.

2 Method and Materials

2.1 Chemicals and materials

Aniline ($\geq 99.0\%$), ammonium persulfate (APS, ACS reagent, $\geq 98.0\%$), polytetrafluoroethylene (PTFE) solution (1% wt) and 2-Hydrox-1,4-naphthoquinone (HNQ, 97%) were purchased from Sigma-Aldrich. Multi-walled CNTs (95%, 10-20nm) were received from Shenzhen Nanotech Co. Ltd. (Shenzhen, China). All other chemicals were of analytical grade and used as received except additional description. Deionized (DI) water (resistance over $18 \text{ M}\Omega \text{ cm}$) from a Millipore Q water purification system was used in all experiments.

2.2 Synthesis of PANI and CNT/PANI composites

Aniline monomer was distilled under reduced pressure before the polymerization. PANI was chemically synthesized as follows: Aniline (1 mL) was mixed with HCl (0.3 mL) in 50 mL deionized (DI) water in an ice bath. Then an APS solution (2.3 g in 25 mL DI water) was added into the mixture. The polymerization was carried out for 6 h in the ice bath ($0-5^\circ\text{C}$). A green solid of proton-doped PANI was obtained after rinsing with DI water for several times. The CNTs were ultrasonically treated using a mixture of 3:1 of H_2SO_4 : HNO_3 at 50°C for 24 h to produce carboxylic acid groups at the defect sites for its improved solubility in HCl solution. The composite of proton-doped PANI/CNT was *in situ* synthesized via chemical oxidation. Different weight ratios of CNT to aniline were used. The CNTs were dissolved in 1.0 M HCl solution first followed by ultrasonic treatment over 3h, and then was transferred into a 250 ml flask placed in the ice-bath. 1.0 M HCl aniline monomer solution was added to the prepared CNT-HCl suspension. Then the APS solution was added into the suspension with constantly stirring at $0-5^\circ\text{C}$ for 6 h-reaction. A precipitate was produced. After filtering and rinsing for several times with DI water and methanol, the precipitate was vacuum-dried at 60°C for 24 h and a powder containing CNT and PANI was obtained, which was ready for preparation of the anode of the MFC.

2.3 Characterization of PANI and CNT/PANI composite

Infrared spectra were recorded using a Fourier transform infrared spectroscopy (Nicolet

MAGNA-IR 560, FTIR, U.S.A.) with an attenuated total reflection (ATR) accessory. The morphology of the plain PANI and the CNT/PANI composite powder was studied with a JEOL 6700 field emission scanning electronic microscopy (FESEM). Nitrogen adsorption isotherms were measured with automated gas sorption system (AUTOSORB-1, Quantachrome Instruments) at the liquid nitrogen temperature. The specific surface area was calculated using Brunauer-Emmett-Teller (BET) method.

2.4 Electrode preparation

The plain PANI and its composite powders were mixed with the PTFE solution to prepare pastes. Then the pastes were coated on the surface of nickel foams (1 cm×1 cm×0.1 cm) to produce uniformly films followed by pressing with a presser to fabricate PANI and CNT/PANI electrodes, respectively. The film covered the whole surface of the nickel foam to prevent the nickel exposure from the electrolyte. After drying at 120°C to remove the water, the electrodes were used as the anodes for MFCs.

2.5 Bacteria growth

Escherichia coli K12 (ATCC 29181) was grown anaerobically at 37°C for 12 h in a standard glucose medium, which was a mixture contained 10 g glucose, 5 g yeast extract, 10 g NaHCO₃ and 8.5 g NaH₂PO₄ per liter. For chronoamperometric measurements, the overnight culture in the above medium was inoculated into fresh anaerobic medium. For impedance and constant current discharge experiments, bacteria culture was harvested by centrifuge at 4°C (6000rpm, 5min). The produced bacteria were washed for three times and then suspended in 0.1M anaerobic phosphate buffer containing 5.5 mM glucose. The concentration of *E. coli* cells was about 10⁹ cells mL⁻¹. Nitrogen was purged into the suspension for 20 min to block the oxygen in the cell before every test.

2.6 Electrochemical measurements

All electrochemical experiments were carried out with PGSTAT30 Autolab system (Ecochemie, Netherlands) in a three electrode cell consisting of the working electrode prepared discussed above,

a saturated calomel electrode (sat. KCl) reference electrode and a platinum wire counter electrode. 2-Hydroxy-1,4-naphthoquinone (HNQ) was chosen as the electron mediator because it could generate higher coulombic output than commonly used mediators such as resazurin or thionine [23]. Except additional description, electrochemical impedance measurements for the PNAI and CNT/PANI composite electrodes were performed over a frequency range of 0.5 Hz – 100 KHz in 0.1M phosphate buffer at open circuit potential and a perturbation signal of 10 mV.

3 Results and discussion

3.1 FTIR spectroscopy and morphology characterization

The FTIR spectra of plain PANI and CNT/PANI composite are shown in Fig 1. The peak at 835 cm^{-1} is attributed to the N–H out-of-plane bending absorption. The peaks at 1500 cm^{-1} and 1600 cm^{-1} can be assigned to the stretching vibration of the quinoid ring and benzenoid ring respectively, which are the characteristic spectra for PANI. The presence and the enhanced relative intensity of the absorption band with a maximum at 1240 cm^{-1} for the composites were very prominent. The spectra are due to the C–N stretching vibration in proton-doped PANI. The fact of the remarkable enhancement of the spectra indicates the formation of C–N coordinate-covalent bonds between the polymer chain and the radical cation CNT fragments [16, 24]. It was observed that the broad band at 1730 cm^{-1} in PANI (C = O vibration) was drastically enhanced for the CNT/PANI composite and even became the most prominent spectra for the 20% wt CNT/PANI powder. The band near 3000 cm^{-1} is due to the C–H stretching absorption. This signal was broad and strong in the composite samples and relatively weak in the plain PANI. This phenomenon was reported recently and explained that sp^2 carbons of carbon nanotubes perturbed the H-bonding environment and then increased the N-H stretch intensity. These results strongly support the formation of CNT/PANI through the chemical oxidation method.

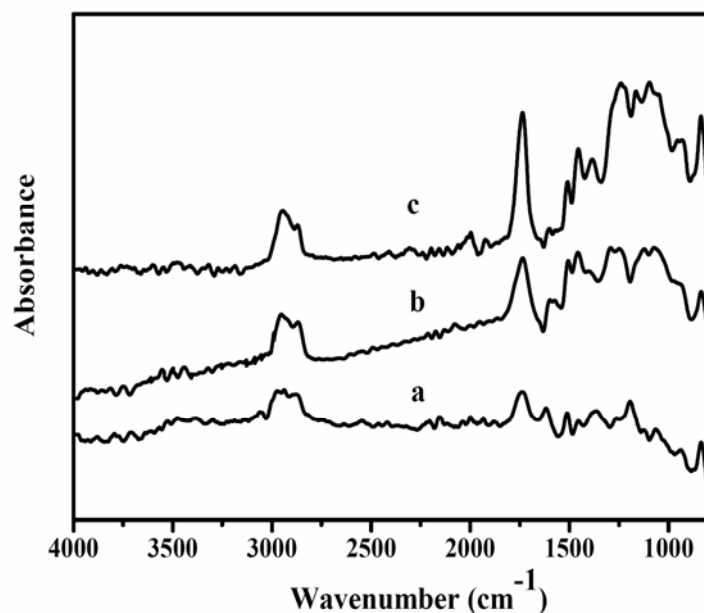


Fig 1. FTIR spectra of PANI and composite powders (a: plain PANI; b: 1% wt CNT/ PANI composite; c: 20% wt CNT/PANI composite)

Figure 2 shows the SEM images of films made from plain PANI and CNT/PANI composite powders. It was illustrated from Figure 2 that the pure PANI film was compact and fibrillar, while the CNT/PANI composite films had a networked-rod nanostructures, in which the outer layer was PANI and the inner layer was constructed by CNTs. The rough, amorphous outer PANI layer had an average thickness of about several tens of nanometers. To verify the effect of CNT doping on the structure of the polymer, the specific surface area of plain PANI and the nanocomposite were measured. The BJH Method Cumulative Adsorption Surface Area of plain PANI was $34.1 \text{ m}^2 \text{ g}^{-1}$. For the nanocomposite, the value was $50.2 \text{ m}^2 \text{ g}^{-1}$. This result proved that the specific surface area of the composite was much larger than the plain polymer. Therefore, it could be expected that the structure difference of these materials could result in different discharge profile and impedance spectra of the anodes made by these materials.

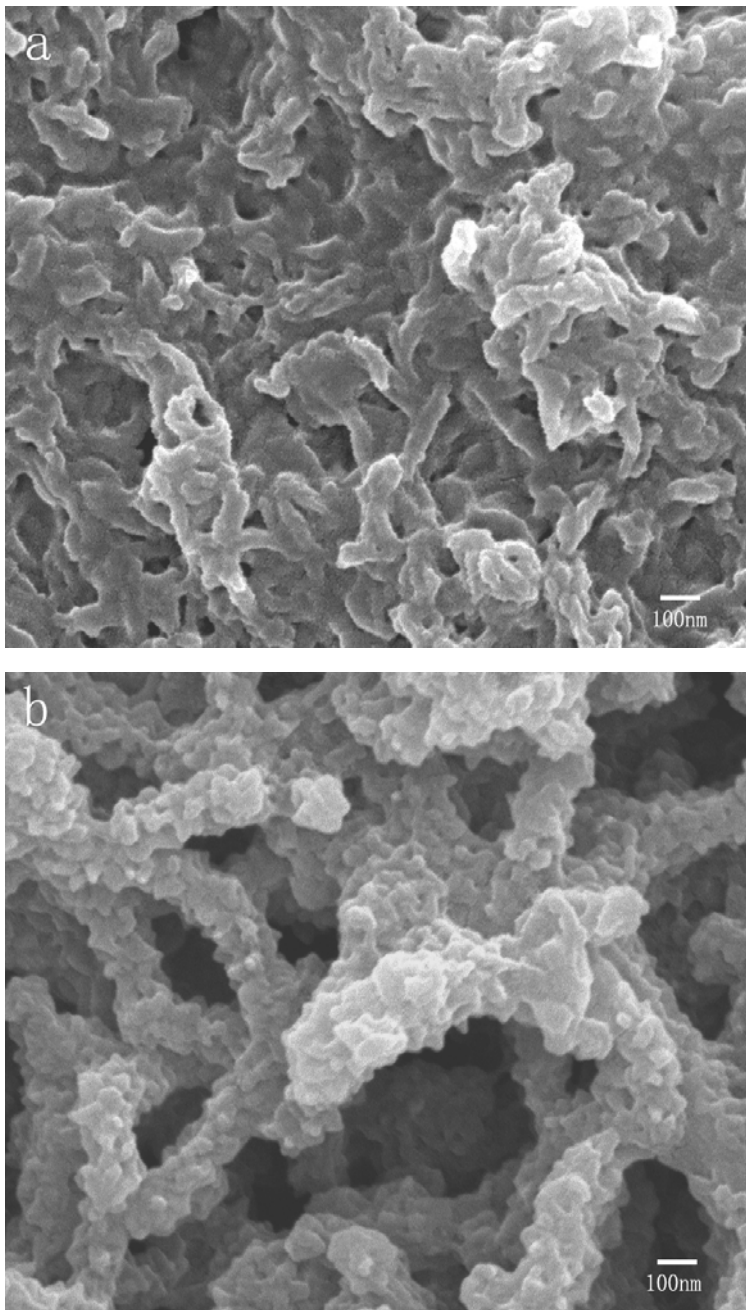
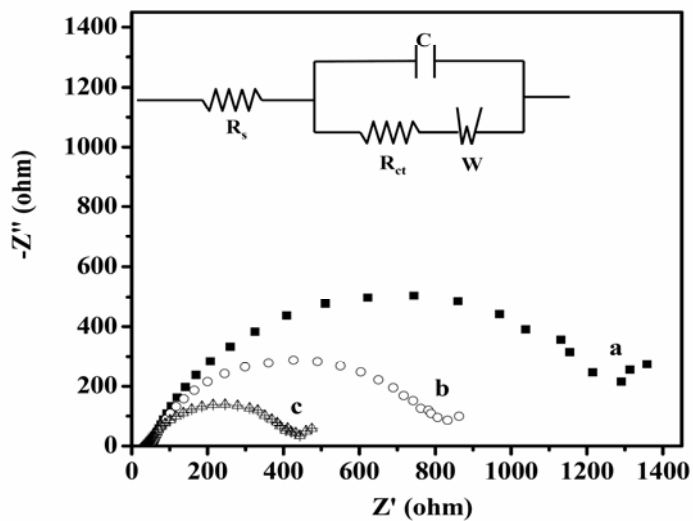


Fig 2. SEM images of PANI and CNT/ PANI composite films. (a: plain PANI; b: 20% wt CNT/ PANI composite)

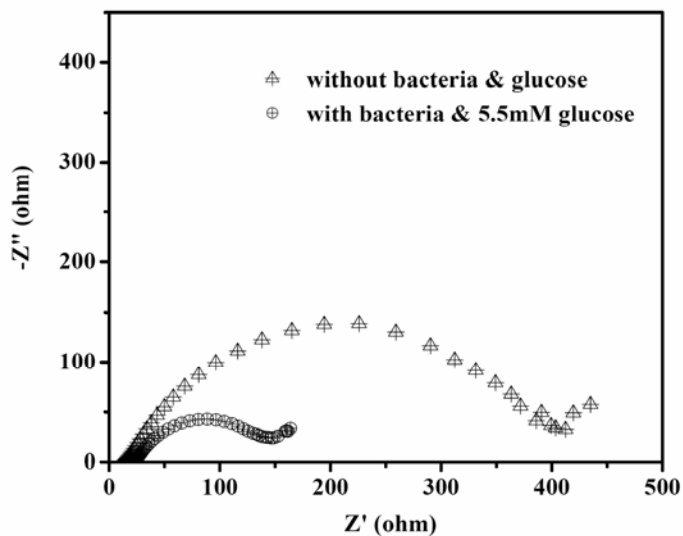
3.2 Electrochemical Impedance Spectra (EIS) studies

Electrochemical impedance spectroscopy (EIS) measurements were carried out to compare the characteristics of charge transfer and ion transport in plain and composite polymers. The measured EIS results (Fig. 3) show well-defined single semi-circles over the high frequency range followed by short straight lines in the low-frequency region for all spectra. Although the impedance spectra showed similar shapes, the diameters of the semicircles declined greatly with the increasing content of CNTs in the polymer film. The diameter of the semicircle corresponds to the interfacial charge-transfer resistance (R_{ct}), which usually represents the resistance of electrochemical reactions on the electrode and is often called as Faraday resistance [25]. In the absence of bacteria and glucose, R_{ct} s of the three electrodes were 1317 (PANI), 827 (1% wt CNT/PANI) and 434 Ω (20% wt CNT/PANI), respectively. Obviously, the R_{ct} of CNT/PANI composite was much lower than that of the pure polyaniline. Since there were no glucose and bacteria in the electrolyte, the R_{ct} should be ascribed to the doping/dedoping redox reactions of PANI. The impedance plane plot in Figure 3 only show very short part of a straight line region, which is an indication of diffusion control for the doping/dedoping process [25]. It is known that the reactants in the doping/dedoping reaction are anions. The narrow region of diffusion controlled process indicated that all tested anodes had good micro/nanostructure for the reactant to access the reaction centers without diffusion limit over a wide frequency range. In a conducting polymer/CNT composite, it has been suggested that either the polymer functionalizes the CNTs, or the conductive polymer are doped with CNTs, and a charge transfer occurs between the two constituents[26], and also suggest that the CNTs have an obvious improvement effect for a faster charge transfer rate than plain PANI. The EIS of 20% wt CNT/PANI electrode in the phosphate buffer in presence of bacteria with and without 5.5mM glucose were also investigated at DC bias of 100mV vs. SCE. The results are shown in Fig 3 (B). When the electrode was tested in the phosphate buffer with both bacteria and glucose, the R_{ct} was about 156 Ω , which was significantly smaller than that in presence of bacteria but without glucose in the electrolyte (400 Ω). As discussed above, the electrochemical reactions without glucose in the solution were caused by doping/dedoping process of PANI. The significant reduction of R_{ct} indicated that the glucose oxidation at such a CNT/PANI/HNQ/*E-coli K12* anode system even had faster reaction rate

than that of doping/dedoping redox reaction. This was very interesting mechanism. The result revealed that the composite anode not only improved the electrode conductivity and specific surface area, but also provided unique active centers, possibly due to its specific nanostructure as shown in Fig. 2b, to host the bacteria for efficient superior electrocatalysis.



(A)



(B)

Fig 3. (A): EIS of PANI (a), 1% wt CNT/PANI (b) and 20% wt CNT/PANI (c) composite electrode in 0.1M phosphate buffer (pH 7) at open circuit potential and the equivalent circuit used to fit the EIS. (B): EIS of 20% wt CNT/PANI in 0.1M phosphate buffer with or without bacteria and glucose; at 100mV vs SCE.

3.3 Anode discharge performance in MFC

In order to evaluate the discharge performance of different anodes in a MFC, an anode limiting beaker MFC was designed, in which a Pt cathode with much larger surface area than that of anodes. Thus, the polarization of the cathode was insignificant. The catalytic current from the glucose oxidation at a constant potential was measured. As shown in Fig. 4, the current increased as the growth and proliferation of the bacteria on the electrode surface. The current-time curves of PANI and composite anodes were significantly different from each other. For plain PANI anode, the current increased very slowly and the current density was much lower than the composites. For the two CNT/PANI composite anodes, when the current of 1% CNT/PANI anode reached a plateau, the current of the 20% CNT/PANI anode was still increasing and the current density was much higher than the former. This could be explained by that the nanocomposite electrodes had more reaction activity sites (larger specific surface area) for the bacteria-catalytic oxidation of glucose and the active sites increased with the increasing of doping amount of CNTs. This result is in agreement with the impedance analysis and the BET results. The constant current discharge experiments of the MFCs comprising the three different anodes in 5.5 mM glucose solution were conducted at 50mA m^{-2} . The results of the anode potentials vs. time (Fig. 5) showed different discharge profiles for the three anodes. Within 180 minutes the discharge potentials for plain PANI, 1%CNT/PANI and 20%CNT/PANI changed from -0.01 to -0.2, -0.36, and -0.38V, respectively. For a fuel cell system, the more negative the anode discharge potential, the higher the operation voltage of the fuel cell. The discharge results that the composite anode could provide higher power density due to its lower polarization, further indicating that the nanostructured composites had faster reaction rate. It was also demonstrated that the composite with higher CNT content (20%) had better discharge performance than that with less CNT content (1%). It was observed that the discharge profile of the bacteria anode was fundamentally different from the conventional anode behavior. The bacteria anode had high polarization potential initially and became lower with the extension of the discharge time. This was due to the bacteria growth process since the discharge process started immediately after addition of glucose solution and bacteria. The bacteria needed time to grow to its maximum and to distribute into the inner surface of the anode as shown in Fig. 4.

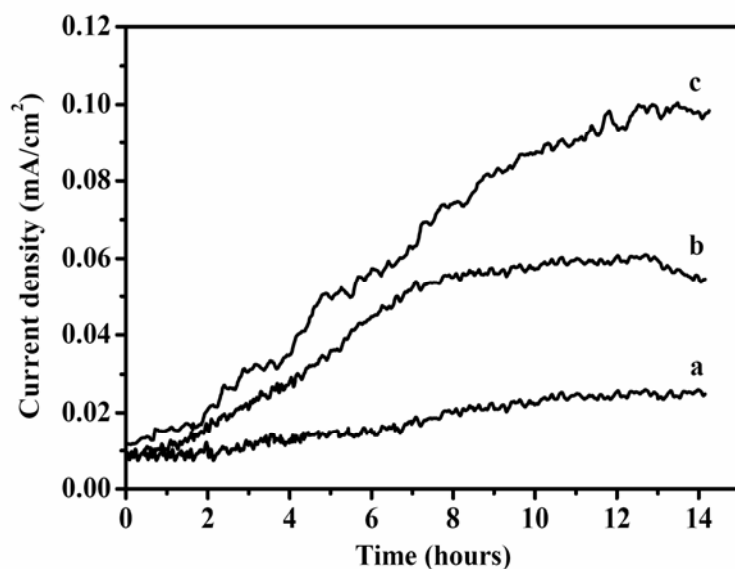


Fig 4. Chronoamperometric plots of PANI and CNT/ PANI composite electrodes placed in a stirred anaerobic culture of *Escherichia coli* K12 in a standard glucose medium. The potential applied to the electrode was 0.1V. Curve a: plain PANI; b: CNT/ PANI composite containing 1% (wt) CNT; c: CNT/ PANI composite containing 20% (wt) CNT

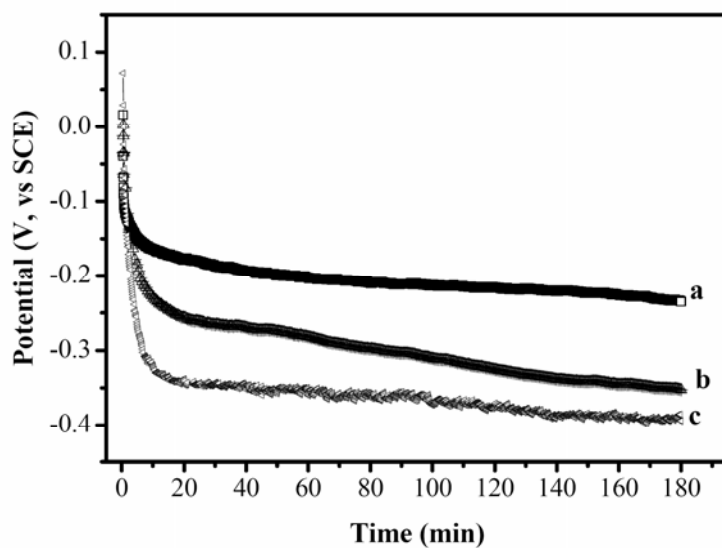


Fig 5. Potential-time curve of PANI and CNT/ PANI composite electrodes placed in a stirred anaerobic culture of *Escherichia coli* K12 in 0.1M phosphate buffer with 5.5mM glucose. Curve a: plain PANI; b: CNT/ PANI composite containing 1% (wt) CNT; c: CNT/ PANI composite containing 20% (wt) CNT

3.4 Power output of the 20% wt CNT/PANI MFC

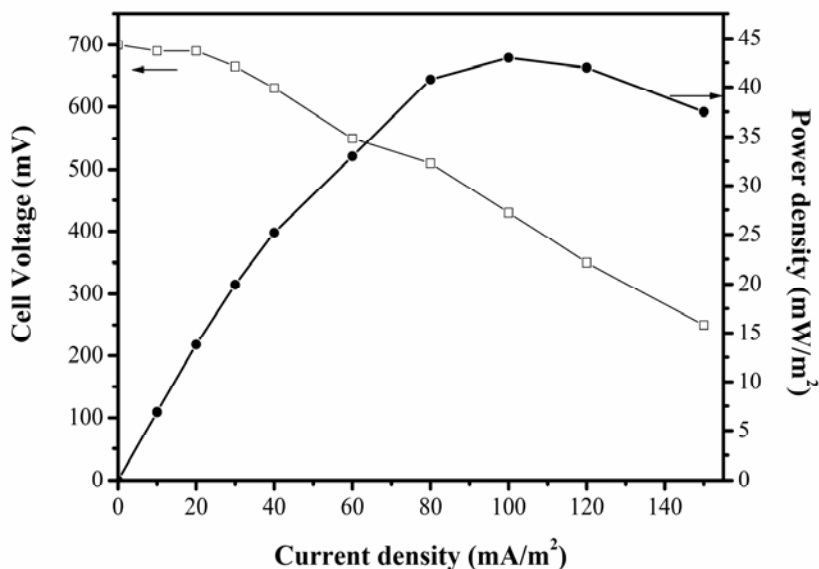


Fig 6. Power output and polarization curve of an anode-limiting MFC with 20% wt CNT/PANI as the anode material

As the 20% wt CNT/PANI MFC showed the best performance in the measurements, we studied its power output and polarization with the anode-limiting MFC. The results are shown in Figure 6. It could be observed from the polarization curve that the cell voltage dropped to 250 mV at the current density of 145 mA m⁻². The power density of the 20% wt CNT/PANI MFC was calculated with the results of chronopotential measurement under different current density. The curve of the power density vs. current density showed a volcano shape. The power density increased with the increase of current density first and reached the maximum value and then sharply dropped with the further increase of current density. Actually, this is the typical relationship of output power density against the current density. The maximum power density was 42 mW m⁻², which was obtained at current density of about 100 mA m⁻² with a cell voltage of 450 mV. It was reported [27] that woven graphite electrodes in *E-coli* microbial fuel cells could deliver maximum power density of 0.47 – 2.6 mW m⁻² with cell voltages of 0.6 – 3.3 V; the power density could reach 91 mW m⁻² with Mn⁴⁺ modified woven graphite as the anode but its cell voltage was about 0.28V. In considering that the

anode thickness of the anode used in our work was smaller than 1 mm in comparison to 1 cm thickness of the anodes used in [27], the CNT/PANI anode demonstrated superior electrocatalytic activity.

4 Conclusions

This work reported that nanostructured CNT/PANI nanocomposite could be used as the anode for a microbial fuel cell. The addition of CNTs in PANI increased the electrode specific surface area and enhanced the charge transfer capability for considerable improvement of the electrochemical activity for the anode reaction in a MFC. The CNT/PANI/*E-coli* K12/HNQ anode system demonstrated much higher power output than that of PANI/*E-coli* K12/HNQ system, showing a superior and specific electrocatalytic effect of the nanocomposite for MFCs in comparison the existing prior arts. The composite containing 20% wt CNT had the best discharge performance to deliver high power output of 42 mW m⁻² with a cell voltage of 450 mV. The CNT doped PANI nanocomposite could have great potential in the MFC anode application.

Reference

1. Logan, B.E., B. Hamelers, R. Rozendal, et al. Environmental Science & Technology, **40**(2006): p. 5181-5192.
2. Bullen, R.A., T.C. Arnot, J.B. Lakeman, et al., Biosensors & Bioelectronics, **21**(2006): p. 2015-2045.
3. Rabaey, K. and W. Verstraete, Trends in Biotechnology, **23**(2005): p. 291-298.
4. Allen, R.M. and H.P. Bennetto, Applied Biochemistry and Biotechnology, **39**(1993): p. 27-40.
5. Chaudhuri, S.K. and D.R. Lovley, Nature Biotechnology, **21**(2003): p. 1229-1232.
6. Liu, H.S., C.J. Song, L. Zhang, et al., Journal of Power Sources, **155**(2006): p. 95-110.
7. Liu, Z.L., X.H. Lin, J.Y. Lee, et al., Langmuir, **18**(2002): p. 4054-4060.
8. Wang, C., M. Waje, X. Wang, et al., Nano Letters, **4**(2004): p. 345-348.
9. Ivnitski, D., B. Branch, P. Atanassov, et al., Electrochemistry Communications, **8**(2006): p.

1204-1210.

10. Yan, Y.M., W. Zheng, L. Su, et al., *Advanced Materials*, **18**(2006): p. 2639-+.
11. Flahaut, E., M.C. Durrieu, M. Remy-Zolghadri, et al., *Journal of Materials Science*, **41**(2006): p. 2411-2416.
12. Magrez, A., S. Kasas, V. Salicio, et al., *Nano Letters*, **6**(2006): p. 1121-1125.
13. Skotheim T.A., R. L. E., J.R. Reynolds, *Handbook of Conducting Polymers*, Dekker, New York 1998.
14. Li C. M., W. Chen, X. Yang, et al., *Frontiers in Bioscience*, **10**(2005): p. 2518-2526..
15. Dong H., C. M. Li., W. Chen, et al., *Anal Chem.*, **8**(2006): p.7424-7431.
16. Huseyin Zengin, W.Z., Jianyong Jin, Richard Czerw, Dennis W. Smith, Jr., Luis Echegoyen, David L. Carroll, Stephen H. Foulger, and John Ballato, *Advanced Materials*, **14**(2002): p. 1480-1483.
17. Muhammad-Tahir, Z. and E.C. Alocilja, *IEEE Sensors Journal*, **3**(2003): p. 345-351.
18. Misra, S.C.K. and R. Angelucci, *Indian Journal of Pure & Applied Physics*, **39**(2001): p. 726-730.
19. Uwe Schroder, J.N., and Fritz Scholz, *Angewandte Chemie*, **115**(2003): p. 2986-2989.
20. Juliane Niessen, U.S., Miriam Rosenbaum, Fritz Scholz, *Electrochemistry Communications*, **6**(2004): p. 571-575.
21. Mottaghitlab, V., G.M. Spinks, and G.G. Wallace, *Synthetic Metals*, **152**(2005): p. 77-80.
22. Liu, J.Y., S.J. Tian, and W. Knoll, *Langmuir*, **21**(2005): p. 5596-5599.
23. Lee, S.A., Y. Choi, S.H. Jung, et al., *Bioelectrochemistry*, **57**(2002): p. 173-178.
24. Raquel Sainz, A.M.B., M. Teresa Martinez, Juan F. Galindo, Javier Sotres, Arturo M. Baro, Benoit Corraze, Olivier Chauvet, and Wolfgang K. Master, *Advanced Materials*, **17**(2005): p. 278-281.
25. Bard, A.J., L.R. Faulkner, *Electrochemical Methods: Fundamentals and Applications*, (2001): Second, editor. New York: Wiley.
26. Guo, D.J. and H.L. Li, *Journal of Solid State Electrochemistry*, **9**(2005): p. 445-449.
27. Park, D.H. and J.G. Zeikus, *Biotechnology and Bioengineering*, **81**(2003): p. 348-355.

Appendix

One manuscript has submitted to Journal of Power Sources, and currently under review.

density could achieve 42 mW m^{-2} with *E. coli* as the microbial catalyst. In comparison to the reported performance of different anodes used in *E. coli*-based MFCs, the CNT/PANI composite anode was excellent, and could have great potential in MFC applications.

Key words: Polyaniline; carbon nanotube; microbial fuel cell; anode modification

1 Introduction

MFCs use bacteria as the catalysts to oxidize organic and inorganic matter for energy generation. A number of factors affect MFC performance including microbial inoculums, chemical substrate, proton exchange material (or absence of this material), cell internal and external resistance, solution ionic strength, electrode materials and electrode spacing [1-3]. Among these factors, a high performance electrode material is most essential. To improve the power output of MFCs, a lot of researchers focus on the cathode modification and bacteria inoculums optimization [4, 5]. However, anode is also important in the performance of a MFC, and is often the limiting factor for a high power output. The anode material and its structure could directly affect the bacteria attachment, electron transfer and substrate oxidation. Up to date, carbon materials such as carbon cloth and carbon paper are applied in most of MFC anodes due to its stability in a microbial inoculum mixture, high conductivity and high specific surface area. Nevertheless, they have no considerable electrocatalysis for the anode microbial reactions and thus the modification of carbon material is the main approach for improving their performance. There is a great need to develop a new-type anode material for MFCs, which is more advantageous than regular carbon cloth and carbon papers.

The CNT is a unique member of the nanostructured carbon materials, which has shown very promising properties as the catalyst support for fuel cell applications due to their unique electrical and structural properties [6]. CNTs were superior to carbon blacks as catalyst supports for proton exchange membrane fuel cells (PEMFCs) [7, 8]. They were also served as anode materials for enzymatic biofuel cells [9, 10]. However, it was reported that CNT had cellular toxicity that could lead to proliferation inhibition and cell death [11, 12]. Thus, it was not suitable for MFCs unless it was modified to reduce the cellular toxicity.

Conductive polymers have attracted intensive research in different electrochemical devices [13-15]. PANI is one of the important conducting polymers due to its relatively facile process ability, electrical conductivity, and environmental stability. The electronic properties of PANI can be reversibly controlled by both doping/dedoping and protonation process, in which its emeraldine base and emeraldine salt form can be interchanged [16]. It was reported that PANI was used to detect microorganism such as *E. coli* with enzyme based method [17, 18]. Uwe et al employed PANI to modify platinum electrode as the anode of MFC. They accomplished a current output more than one order of magnitude larger than the known MFCs [19]. The conductive PANI used in the MFC not only has a protective function for bacteria, but also directly contributes to electrocatalysis with a high current density [19, 20]. However, the lower conductivity and poor electron transfer of PANI limit its application in MFCs.

The fabrication of CNT/PANI composites has received great interest in recent years since the incorporation of CNTs into PANI can result in new composite materials with enhanced electronic properties. For example, Wallace et al. reported that the PANI fibers containing CNTs exhibited significant improvement in mechanical strength and conductivity [21]. Liu et al. constructed CNT/PANI multilayer films through the layer-by-layer assembly method, and the CNTs inside the multilayer film could expand the electroactivity of PANI to a neutral electrolyte [22]. Thus, the enhanced conductive CNT/PANI composite could possibly be used in MFCs for performance improvement. However, the electrocatalytic behavior and application of the CNT/PANI composite in MFCs has not been studied. In this report, we used the CNT/PANI composite as the anode of MFCs for the first time and investigated the electrocatalytic properties of the composite associated with the bacterium biocatalyst. A method was developed to fabricate a nanostructured CNT/PANI composite anode for MFCs. In our experiments, anaerobic cultured *Escherichia coli K12* was used as the biological catalyst and glucose was used as the organic substrate for the anode-limiting MFC cell. The discharge performance of the CNT/PANI anode in the testing MFC was evaluated with the beaker MFC.

2 Method and Materials

2.1 Chemicals and materials

Aniline ($\geq 99.0\%$), ammonium persulfate (APS, ACS reagent, $\geq 98.0\%$), polytetrafluoroethylene (PTFE) solution (1% wt) and 2-Hydrox-1,4-naphthoquinone (HNQ, 97%) were purchased from Sigma-Aldrich. Multi-walled CNTs (95%, 10-20nm) were received from Shenzhen Nanotech Co.

Ltd. (Shenzhen, China). All other chemicals were of analytical grade and used as received except additional description. Deionized (DI) water (resistance over 18 M Ω cm) from a Millipore Q water purification system was used in all experiments.

2.2 Synthesis of PANI and CNT/PANI composites

Aniline monomer was distilled under reduced pressure before the polymerization. PANI was chemically synthesized as follows: Aniline (1 mL) was mixed with HCl (0.3 mL) in 50 mL deionized (DI) water in an ice bath. Then an APS solution (2.3 g in 25 mL DI water) was added into the mixture. The polymerization was carried out for 6 h in the ice bath (0–5°C). A green solid of proton-doped PANI was obtained after rinsing with DI water for several times. The CNTs were ultrasonically treated using a mixture of 3:1 of H₂SO₄ : HNO₃ at 50°C for 24 h to produce carboxylic acid groups at the defect sites for its improved solubility in HCl solution. The composite of proton-doped PANI/CNT was *in situ* synthesized via chemical oxidation. Different weight ratios of CNT to aniline were used. The CNTs were dissolved in 1.0 M HCl solution first followed by ultrasonic treatment over 3h, and then was transferred into a 250 ml flask placed in the ice-bath. 1.0 M HCl aniline monomer solution was added to the prepared CNT-HCl suspension. Then the APS solution was added into the suspension with constantly stirring at 0–5°C for 6 h-reaction. A precipitate was produced. After filtering and rinsing for several times with DI water and methanol, the precipitate was vacuum-dried at 60°C for 24 h and a powder containing CNT and PANI was obtained, which was ready for preparation of the anode of the MFC.

2.3 Characterization of PANI and CNT/PANI composite

Infrared spectra were recorded using a Fourier transform infrared spectroscopy (Nicolet MAGNA-IR 560, FTIR, U.S.A.) with an attenuated total reflection (ATR) accessory. The morphology of the plain PANI and the CNT/PANI composite powder was studied with a JEOL 6700 field emission scanning electronic microscopy (FESEM). Nitrogen adsorption isotherms were measured with automated gas sorption system (AUTOSORB-1, Quantachrome Instruments) at the liquid nitrogen temperature. The specific surface area was calculated using Brunauer-Emmett-Teller (BET) method.

2.4 Electrode preparation

The plain PANI and its composite powders were mixed with the PTFE solution to prepare pastes. Then the pastes were coated on the surface of nickel foams (1 cm×1 cm×0.1 cm) to produce uniformly films followed by pressing with a presser to fabricate PANI and CNT/PANI electrodes, respectively. The film covered the whole surface of the nickel foam to prevent the nickel exposure from the electrolyte. After drying at 120°C to remove the water, the electrodes were used as the anodes for MFCs.

2.5 Bacteria growth

Escherichia coli K12 (ATCC 29181) was grown anaerobically at 37°C for 12 h in a standard glucose medium, which was a mixture contained 10 g glucose, 5 g yeast extract, 10 g NaHCO₃ and 8.5 g NaH₂PO₄ per liter. For chronoamperometric measurements, the overnight culture in the above

medium was inoculated into fresh anaerobic medium. For impedance and constant current discharge experiments, bacteria culture was harvested by centrifuge at 4°C (6000rpm, 5min). The produced bacteria were washed for three times and then suspended in 0.1M anaerobic phosphate buffer containing 5.5 mM glucose. The concentration of *E. coli* cells was about 10^9 cells mL⁻¹. Nitrogen was purged into the suspension for 20 min to block the oxygen in the cell before every test.

2.6 Electrochemical measurements

All electrochemical experiments were carried out with PGSTAT30 Autolab system (Ecochemie, Netherlands) in a three electrode cell consisting of the working electrode prepared discussed above, a saturated calomel electrode (sat. KCl) reference electrode and a platinum wire counter electrode. 2-Hydroxy-1,4-naphthoquinone (HNQ) was chosen as the electron mediator because it could generate higher coulombic output than commonly used mediators such as resazurin or thionine [23]. Except additional description, electrochemical impedance measurements for the PNAI and CNT/PANI composite electrodes were performed over a frequency range of 0.5 Hz – 100 KHz in 0.1M phosphate buffer at open circuit potential and a perturbation signal of 10 mV..

3 Results and discussion

3.1 FTIR spectroscopy and morphology characterization

The FTIR spectra of plain PANI and CNT/PANI composite are shown in Fig 1. The peak at 835 cm⁻¹ is attributed to the N–H out-of-plane bending absorption. The peaks at 1500 cm⁻¹ and 1600 cm⁻¹ can be assigned to the stretching vibration of the quinoid ring and benzenoid ring respectively, which

are the characteristic spectra for PANI. The presence and the enhanced relative intensity of the absorption band with a maximum at 1240 cm^{-1} for the composites were very prominent. The spectra are due to the C-N stretching vibration in proton-doped PANI. The fact of the remarkable enhancement of the spectra indicates the formation of C-N coordinate-covalent bonds between the polymer chain and the radical cation CNT fragments [16, 24]. It was observed that the broad band at 1730 cm^{-1} in PANI (C = O vibration) was drastically enhanced for the CNT/PANI composite and even became the most prominent spectra for the 20% wt CNT/PANI powder. The band near 3000 cm^{-1} is due to the C-H stretching absorption. This signal was broad and strong in the composite samples and relatively weak in the plain PANI. This phenomenon was reported recently and explained that sp^2 carbons of carbon nanotubes perturbed the H-bonding environment and then increased the N-H stretch intensity. These results strongly support the formation of CNT/PANI through the chemical oxidation method.

Figure 2 shows the SEM images of films made from plain PANI and CNT/PANI composite powders. It was illustrated from Figure 2 that the pure PANI film was compact and fibrillar, while the CNT/PANI composite films had a networked-rod nanostructures, in which the outer layer was PANI and the inner layer was constructed by CNTs. The rough, amorphous outer PANI layer had an average thickness of about several tens of nanometers. To verify the effect of CNT doping on the structure of the polymer, the specific surface area of plain PANI and the nanocomposite were measured. The BJH Method Cumulative Adsorption Surface Area of plain PANI was $34.1\text{ m}^2\text{ g}^{-1}$. For the nanocomposite, the value was $50.2\text{ m}^2\text{ g}^{-1}$. This result proved that the specific surface area of the composite was much larger than the plain polymer. Therefore, it could be expected that the

structure difference of these materials could result in different discharge profile and impedance spectra of the anodes made by these materials.

3.2 Electrochemical Impedance Spectra (EIS) studies

Electrochemical impedance spectroscopy (EIS) measurements were carried out to compare the characteristics of charge transfer and ion transport in plain and composite polymers. The measured EIS results (Fig. 3) show well-defined single semi-circles over the high frequency range followed by short straight lines in the low-frequency region for all spectra. Although the impedance spectra showed similar shapes, the diameters of the semicircles declined greatly with the increasing content of CNTs in the polymer film. The diameter of the semicircle corresponds to the interfacial charge-transfer resistance (R_{ct}), which usually represents the resistance of electrochemical reactions on the electrode and is often called as Faraday resistance [25]. In the absence of bacteria and glucose, R_{ct} s of the three electrodes were 1317 (PANI), 827 (1% wt CNT/PANI) and 434 Ω (20% wt CNT/PANI), respectively. Obviously, the R_{ct} of CNT/PANI composite was much lower than that of the pure polyaniline. Since there were no glucose and bacteria in the electrolyte, the R_{ct} should be ascribed to the doping/dedoping redox reactions of PANI. The impedance plane plot in Figure 3 only show very short part of a straight line region, which is an indication of diffusion control for the doping/dedoping process [25]. It is known that the reactants in the doping/dedoping reaction are anions. The narrow region of diffusion controlled process indicated that all tested anodes had good micro/nanostructure for the reactant to access the reaction centers without diffusion limit over a wide frequency range. In a conducting polymer/CNT composite, it has been suggested that either the

polymer functionalizes the CNTs, or the conductive polymer are doped with CNTs, and a charge transfer occurs between the two constituents[26], and also suggest that the CNTs have an obvious improvement effect for a faster charge transfer rate than plain PANI. The EIS of 20% wt CNT/PANI electrode in the phosphate buffer in presence of bacteria with and without 5.5mM glucose were also investigated at DC bias of 100mV vs. SCE. The results are shown in Fig 3 (B). When the electrode was tested in the phosphate buffer with both bacteria and glucose, the R_{ct} was about 156 Ω , which was significantly smaller than that in presence of bacteria but without glucose in the electrolyte (400 Ω). As discussed above, the electrochemical reactions without glucose in the solution were caused by doping/dedoping process of PANI. The significant reduction of R_{ct} indicated that the glucose oxidation at such a CNT/PANI/HNQ/*E-coli K12* anode system even had faster reaction rate than that of doping/dedoping redox reaction. This was very interesting mechanism. The result revealed that the composite anode not only improved the electrode conductivity and specific surface area, but also provided unique active centers, possibly due to its specific nanostructure as shown in Fig. 2b, to host the bacteria for efficient superior electrocatalysis.

3.3 Anode discharge performance in MFC

In order to evaluate the discharge performance of different anodes in a MFC, an anode limiting beaker MFC was designed, in which a Pt cathode with much larger surface area than that of anodes. Thus, the polarization of the cathode was insignificant. The catalytic current from the glucose oxidation at a constant potential was measured. As shown in Fig. 4, the current increased as the growth and proliferation of the bacteria on the electrode surface. The current-time curves of PANI

and composite anodes were significantly different from each other. For plain PANI anode, the current increased very slowly and the current density was much lower than the composites. For the two CNT/PANI composite anodes, when the current of 1% CNT/PANI anode reached a plateau, the current of the 20% CNT/PANI anode was still increasing and the current density was much higher than the former. This could be explained by that the nanocomposite electrodes had more reaction activity sites (larger specific surface area) for the bacteria-catalytic oxidation of glucose and the active sites increased with the increasing of doping amount of CNTs. This result is in agreement with the impedance analysis and the BET results. The constant current discharge experiments of the MFCs comprising the three different anodes in 5.5 mM glucose solution were conducted at 50mA m^{-2} . The results of the anode potentials vs. time (Fig. 5) showed different discharge profiles for the three anodes. Within 180 minutes the discharge potentials for plain PANI, 1%CNT/PANI and 20%CNT/PANI changed from -0.01 to -0.2, -0.36, and -0.38V, respectively. For a fuel cell system, the more negative the anode discharge potential, the higher the operation voltage of the fuel cell. The discharge results that the composite anode could provide higher power density due to its lower polarization, further indicating that the nanostructured composites had faster reaction rate. It was also demonstrated that the composite with higher CNT content (20%) had better discharge performance than that with less CNT content (1%). It was observed that the discharge profile of the bacteria anode was fundamentally different from the conventional anode behavior. The bacteria anode had high polarization potential initially and became lower with the extension of the discharge time. This was due to the bacteria growth process since the discharge process started immediately after addition of glucose solution and bacteria. The bacteria needed time to grow to its maximum

and to distribute into the inner surface of the anode as shown in Fig. 4.

3.4 Power output of the 20% wt CNT/PANI MFC

As the 20% wt CNT/PANI MFC showed the best performance in the measurements, we studied its power output and polarization with the anode-limiting MFC. The results are shown in Figure 6. It could be observed from the polarization curve that the cell voltage dropped to 250 mV at the current density of 145 mA m⁻². The power density of the 20% wt CNT/PANI MFC was calculated with the results of chronopotential measurement under different current density. The curve of the power density vs. current density showed a volcano shape. The power density increased with the increase of current density first and reached the maximum value and then sharply dropped with the further increase of current density. Actually, this is the typical relationship of output power density against the current density. The maximum power density was 42 mW m⁻², which was obtained at current density of about 100 mA m⁻² with a cell voltage of 450 mV. It was reported [27] that woven graphite electrodes in *E-coli* microbial fuel cells could deliver maximum power density of 0.47 – 2.6 mW m⁻² with cell voltages of 0.6 – 3.3 V; the power density could reach 91 mW m⁻² with Mn⁴⁺ modified woven graphite as the anode but its cell voltage was about 0.28V. In considering that the anode thickness of the anode used in our work was smaller than 1 mm in comparison to 1 cm thickness of the anodes used in [27], the CNT/PANI anode demonstrated superior electrocatalytic activity.

4 Conclusions

This work reported that nanostructured CNT/PANI nanocomposite could be used as the anode

for a microbial fuel cell. The addition of CNTs in PANI increased the electrode specific surface area and enhanced the charge transfer capability for considerable improvement of the electrochemical activity for the anode reaction in a MFC. The CNT/PANI/*E-coli* K12/HNQ anode system demonstrated much higher power output than that of PANI/*E-coli* K12/HNQ system, showing a superior and specific electrocatalytic effect of the nanocomposite for MFCs in comparison the existing prior arts. The composite containing 20% wt CNT had the best discharge performance to deliver high power output of 42 mW m⁻² with a cell voltage of 450 mV. The CNT doped PANI nanocomposite could have great potential in the MFC anode application.

4 Acknowledgement

The authors are grateful to the Asian Office of Aerospace Research and Development, Department of The Air Force of USA for the financial support to this work under contract of AOARD-05-4073.

Reference

1. Logan, B.E., B. Hamelers, R. Rozendal, et al. *Environmental Science & Technology*, **40**(2006): p. 5181-5192.
2. Bullen, R.A., T.C. Arnot, J.B. Lakeman, et al., *Biosensors & Bioelectronics*, **21**(2006): p. 2015-2045.
3. Rabaey, K. and W. Verstraete, *Trends in Biotechnology*, **23**(2005): p. 291-298.
4. Allen, R.M. and H.P. Bennetto, *Applied Biochemistry and Biotechnology*, **39**(1993): p. 27-40.

5. Chaudhuri, S.K. and D.R. Lovley, *Nature Biotechnology*, **21**(2003): p. 1229-1232.
6. Liu, H.S., C.J. Song, L. Zhang, et al., *Journal of Power Sources*, **155**(2006): p. 95-110.
7. Liu, Z.L., X.H. Lin, J.Y. Lee, et al., *Langmuir*, **18**(2002): p. 4054-4060.
8. Wang, C., M. Waje, X. Wang, et al., *Nano Letters*, **4**(2004): p. 345-348.
9. Ivnitski, D., B. Branch, P. Atanassov, et al., *Electrochemistry Communications*, **8**(2006): p. 1204-1210.
10. Yan, Y.M., W. Zheng, L. Su, et al., *Advanced Materials*, **18**(2006): p. 2639-+.
11. Flahaut, E., M.C. Durrieu, M. Remy-Zolghadri, et al., *Journal of Materials Science*, **41**(2006): p. 2411-2416.
12. Magrez, A., S. Kasas, V. Salicio, et al., *Nano Letters*, **6**(2006): p. 1121-1125.
13. Skotheim T.A., R. L. E., J.R. Reynolds, *Handbook of Conducting Polymers*, Dekker, New York 1998.
14. Li C. M., W. Chen, X. Yang, et al., *Frontiers in Bioscience*, **10**(2005): p. 2518-2526..
15. Dong H., C. M. Li., W. Chen, et al., *Anal Chem.*, **8**(2006): p.7424-7431.
16. Huseyin Zengin, W.Z., Jianyong Jin, Richard Czerw, Dennis W. Smith, Jr., Luis Echegoyen, David L. Carroll, Stephen H. Foulger, and John Ballato, *Advanced Materials*, **14**(2002): p. 1480-1483.
17. Muhammad-Tahir, Z. and E.C. Alocilja, *IEEE Sensors Journal*, **3**(2003): p. 345-351.
18. Misra, S.C.K. and R. Angelucci, *Indian Journal of Pure & Applied Physics*, **39**(2001): p. 726-730.
19. Uwe Schroder, J.N., and Fritz Scholz, *Angewandte Chemie*, **115**(2003): p. 2986-2989.

20. Juliane Niessen, U.S., Miriam Rosenbaum, Fritz Scholz, *Electrochemistry Communications*, **6**(2004): p. 571-575.
21. Mottaghitlab, V., G.M. Spinks, and G.G. Wallace, *Synthetic Metals*, **152**(2005): p. 77-80.
22. Liu, J.Y., S.J. Tian, and W. Knoll, *Langmuir*, **21**(2005): p. 5596-5599.
23. Lee, S.A., Y. Choi, S.H. Jung, et al., *Bioelectrochemistry*, **57**(2002): p. 173-178.
24. Raquel Sainz, A.M.B., M. Teresa Martinez, Juan F. Galindo, Javier Sotres, Arturo M. Baro, Benoit Corraze, Olivier Chauvet, and Wolfgang K. Master, *Advanced Materials*, **17**(2005): p. 278-281.
25. Bard, A.J., L.R. Faulkner, *Electrochemical Methods: Fundamentals and Applications*, (2001):
Second, editor. New York: Wiley.
26. Guo, D.J. and H.L. Li, *Journal of Solid State Electrochemistry*, **9**(2005): p. 445-449.
27. Park, D.H. and J.G. Zeikus, *Biotechnology and Bioengineering*, **81**(2003): p. 348-355.

Figures

Captions for Figures

Fig 1. FTIR spectra of PANI and composite powders (a: plain PANI; b: 1% wt CNT/ PANI composite; c: 20% wt CNT/PANI composite)

Fig 2. SEM images of PANI and CNT/ PANI composite films. (a: plain PANI; b: 20% wt CNT/ PANI composite)

Fig 3. (A): EIS of PANI (a), 1% wt CNT/PANI (b) and 20% wt CNT/PANI (c) composite electrode in 0.1M phosphate buffer (pH 7) at open circuit potential and the equivalent circuit used to fit the EIS. (B): EIS of 20% wt CNT/PANI in 0.1M phosphate buffer with or without bacteria and glucose; at 100mV vs SCE.

Fig 4. Chronoamperometric plots of PANI and CNT/ PANI composite electrodes placed in a stirred anaerobic culture of *Escherichia coli* K12 in a standard glucose medium. The potential applied to the electrode was 0.1V. Curve a: plain PANI; b: CNT/ PANI composite containing 1% (wt) CNT; c: CNT/ PANI composite containing 20% (wt) CNT

Fig 5. Potential-time curve of PANI and CNT/ PANI composite electrodes placed in a stirred anaerobic culture of *Escherichia coli* K12 in 0.1M phosphate buffer with 5.5mM glucose. Curve a: plain PANI; b: CNT/ PANI composite containing 1% (wt) CNT; c: CNT/ PANI composite containing 20% (wt) CNT

Fig 6. Power output and polarization curve of the MFC with 20% wt CNT/PANI anode.

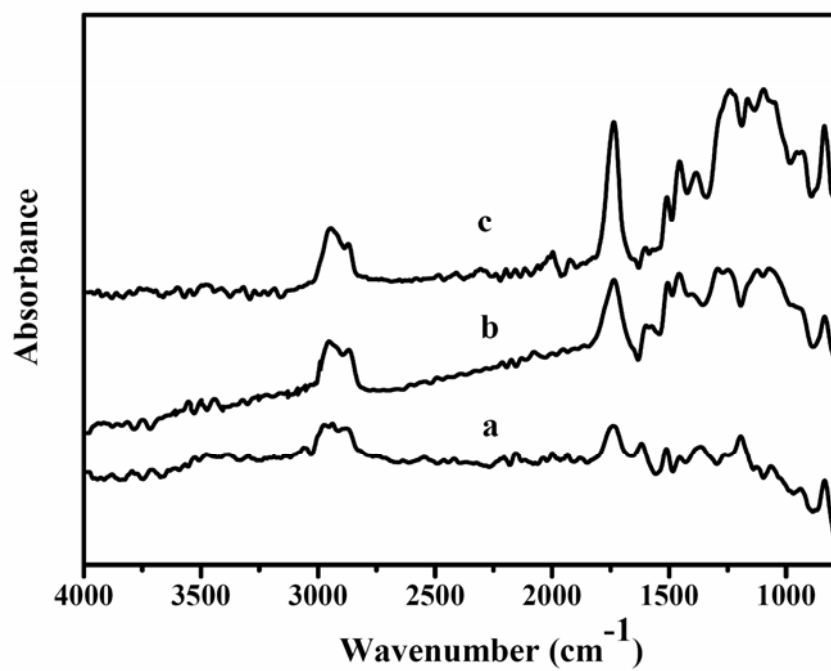


Fig 1. FTIR spectra of PANI and composite powders (a: plain PANI; b: 1% wt CNT/ PANi composite; c: 20% wt CNT/PANI composite)

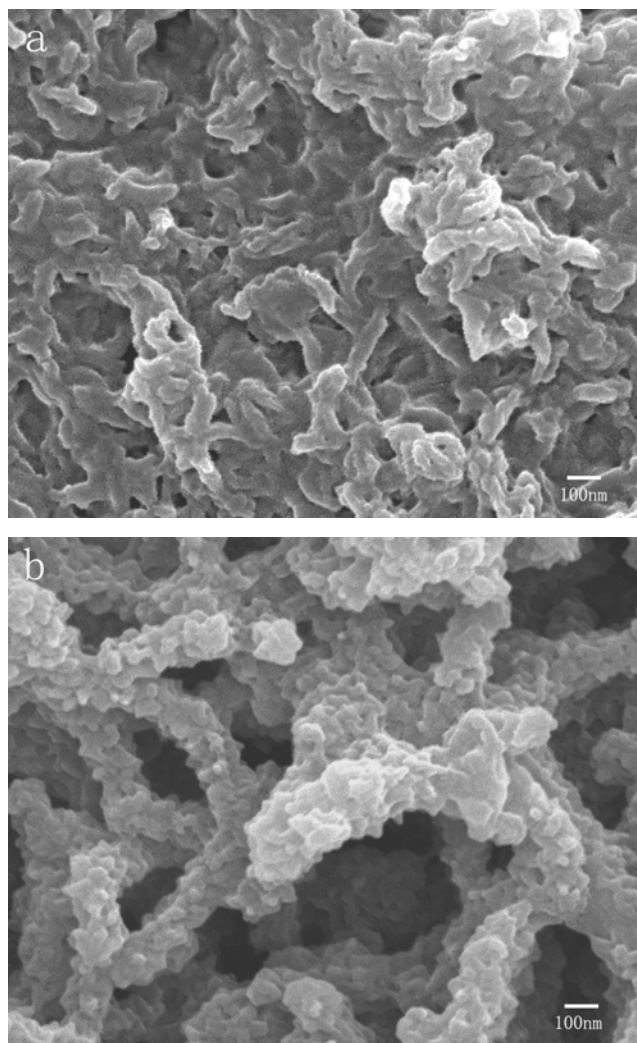
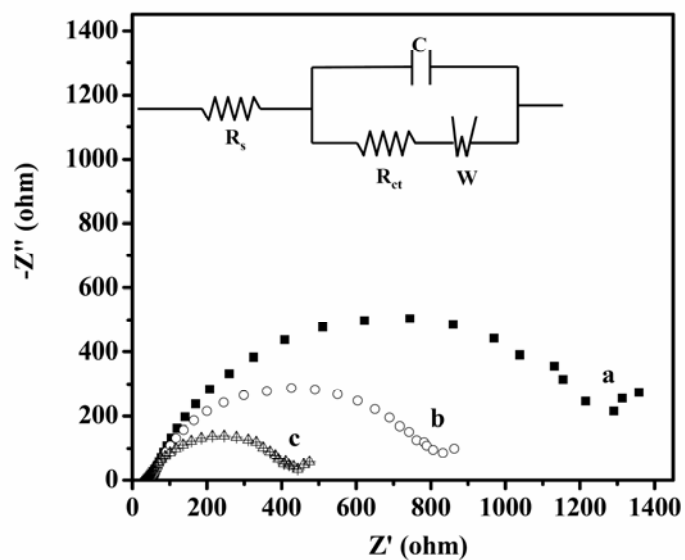
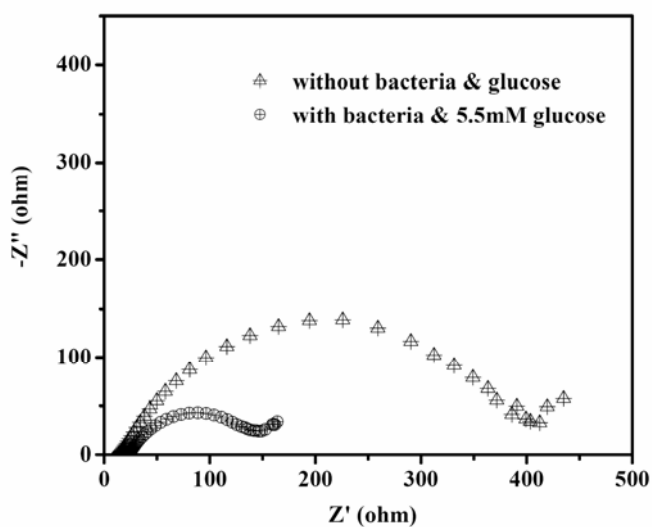


Fig 2. SEM images of PANI and CNT/ PANI composite films. (a: plain PANI; b: 20% wt CNT/ PANI composite)



(A)



(B)

Fig 3. (A): EIS of PANI (a), 1% wt CNT/PANI (b) and 20% wt CNT/PANI (c) composite electrode in 0.1M phosphate buffer (pH 7) at open circuit potential and the equivalent circuit used to fit the EIS. (B): EIS of 20% wt CNT/PANI in 0.1M phosphate buffer with or without bacteria and glucose; at 100mV vs SCE.

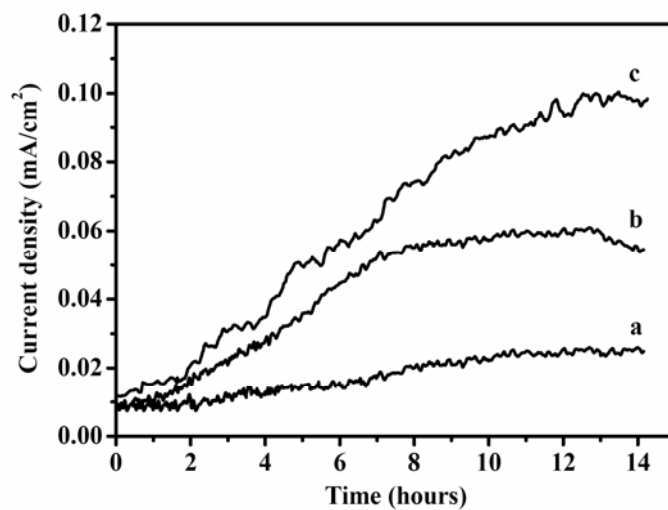


Fig 4. Chronoamperometric plots of PANI and CNT/ PANI composite electrodes placed in a stirred anaerobic culture of *Escherichia coli* K12 in a standard glucose medium. The potential applied to the electrode was 0.1V. Curve a: plain PANI; b: CNT/ PANI composite containing 1% (wt) CNT; c: CNT/ PANI composite containing 20% (wt) CNT

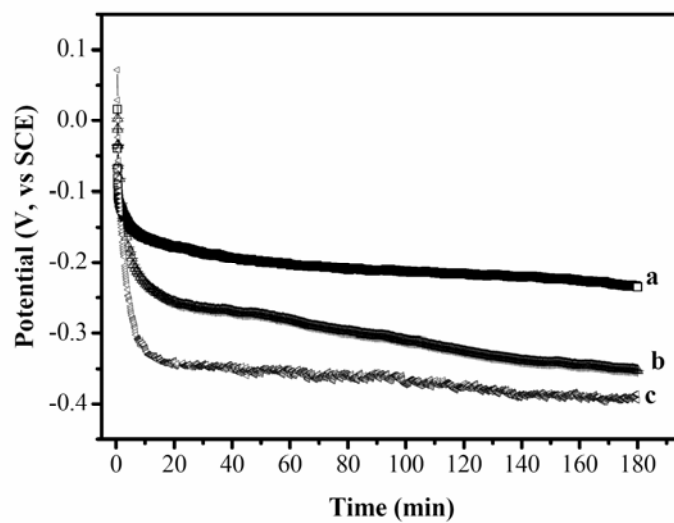


Fig 5. Potential-time curve of PANI and CNT/ PANI composite electrodes placed in a stirred anaerobic culture of *Escherichia coli* K12 in 0.1M phosphate buffer with 5.5mM glucose. Curve a: plain PANI; b: CNT/ PANI composite containing 1% (wt) CNT; c: CNT/ PANI composite containing 20% (wt) CNT

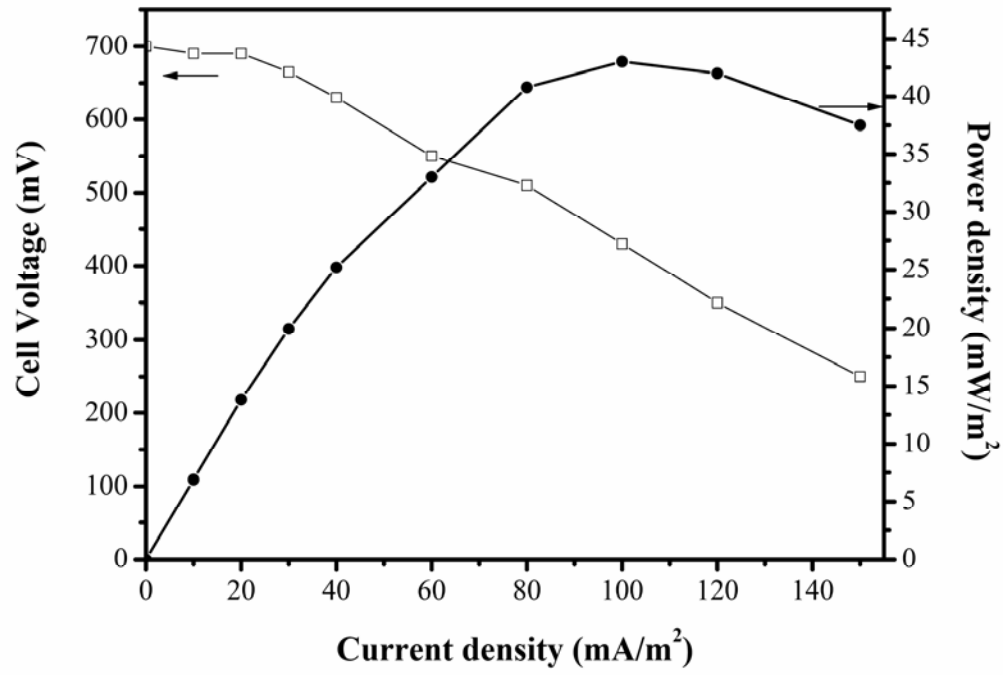


Fig 6. Power output and polarization curve of an anode-limiting MFC with 20% wt CNT/PANI as the anode material